VALIDATION OF SHORT AND MEDIUM TERM OPERATIONAL SOLAR RADIATION FORECASTS IN THE US

Richard Perez, Sergey Kivalov, James Schlemmer, Karl Hemker Jr.,

ASRC, University at Albany

David Renné

National Renewable Energy Laboratory

Thomas E. Hoff

Clean Power Research

ABSTRACT

This paper presents a validation of the short and medium term global irradiance forecasts that are produced as part of the US SolarAnywhere (2010) data set. The short term forecasts that extend up to six-hours ahead are based upon cloud motion derived from consecutive geostationary satellite images. The medium term forecasts extend up to six days ahead and are modeled from gridded cloud cover forecasts from the US National Digital Forecast Database.

The forecast algorithms are validated against ground measurements for seven climatically distinct locations in the United States for one year. An initial analysis of regional performance using satellite-derived irradiances as a benchmark reference is also presented.

1. INTRODUCTION

There are two basic approaches to solar radiation forecasting.

The first approach consists of numerical weather prediction (NWP) models. NWP models can be global -- e.g., GFS (2003), ECMWF (2010) – regional, or local -- e.g., WRF, (2010). For irradiance predictions, the NWP forecasts are inherently probabilistic because they infer local cloud formation probability (and indirectly transmitted radiation) through dynamic modeling of the atmosphere. NWP models cannot, at this stage of their development, predict the exact position and extent of individual clouds or cloud fields affecting a given location's solar resource.

The second approach consists of projecting observed solar radiation conditions based on immediate measured history: The position and impact of future clouds is inferred from their motion determined from recent observations; these observations can be either remote (from satellites) or from appropriate ground based sky-imaging instrumentation (e.g., Slater et al., 2001). This approach is initially deterministic because the initial position of clouds affecting a solar installation is precisely known.

Lorenz et al. (2007) have shown that the cloud-motion based forecasts tend to provide better results than NWP forecasts up to forecast horizons of 3-4 hours, beyond which NWP models perform better.

In this article, we evaluate the NWP-based and satellite-derived cloud motion forecast models producing the SolarAnywhere's hourly global horizontal irradiance (GHI) forecasts.

2. FORECAST MODELS

2.1 Numerical Weather Prediction Forecasts (same day to six days ahead)

The GHI forecasts analyzed here are derived from the US National Digital Forecast Database (NDFD, 2010). The NDFD produces gridded forecasts of a sky cover fraction . The NDFD sky cover forecasts are the result of a multistep forecasting process, involving:

(1) Global NWP modeling from NOAA's GFS model (2003) which estimates sky cover from predicted relative humidity at several elevations (Xu and Randall, 1996),

(2) Modifications of the GFS forecast by regional NOAA offices using a variety of tools including regional/local models and human input; and,

(3) Reassembling of the regional NOAA offices' modified forecasts into a national grid.

The NDFD forecasts are produced on a 3-hourly basis for up to three days ahead and on a 6-hourly basis up to six days ahead. Under normal operating conditions, forecasts are updated hourly. All forecasts analyzed in this paper originate at 11:00 GMT. The NDFD grid is subsampled down to the grid size of SolarAnynywhere: 0.1 x 0.1 degrees in latitude and longitude.

NDFD-derived irradiances are produced using a multi-site empirical fit between the NDFD sky cover and measured GHI indices (see Perez et al., 2007). The hourly GHI forecasts are extracted by time-interpolating the 3-hourly or 6-hourly sky cover forecasts before applying the cloud-amount-to-GHI conversion. For the present study the sky cover to irradiance fit was adjusted, also empirically, to match a subsample of the observations at the seven considered ground-truth locations -- using the first 4 months out of 12 months worth of measurements. This adjustment was made to account for a tendency towards sky cover underprediction as the forecasts time horizon increases to six days -- the

semi-empirical sky-cover-to-irradiance fit presented in Perez et al., (2007)had been based on 1-3 day forecasts only.

2.2 Cloud Motion Forecasts (one to six hours ahead)

The short-term irradiance forecasts are produced using two consecutive satellite-derived GHI index images (Perez et al., 2002, 2004) from which pixel-specific cloud motion is determined. The GHI index, Kt*, is the ratio between GHI and local clear sky global irradiance GHI_{clear}. Future images, up to six hours ahead, are derived from this localized motion. The methodology to determine localized cloud motion was patterned after Lorenz et al. (2007), whereby pixel-specific motion vectors are determined by calculating the RMSE of the difference between two consecutive Kt*grids surrounding the considered pixel when the second grid is advected in the direction of a motion vector. The selected motion vector corresponds to the lowest RMSE. This process is repeated for each image pixel, and each pixel is assigned an individual motion vector. Future images are obtained by displacing the current image pixels in the direction of their motion vector. Future images are subsequently smoothed by averaging each pixel with its 8 surrounding neighbors following the pragmatic approach described by Lorenz et al. (2007).

3. VALIDATION

Forecasts are validated against single-point ground-truth stations. In addition, the ability of forecast models to account for local microclimatology is investigated by observing the distribution of mean predictions over extended areas.

3.1 Single Point Ground-Truth Validation

Hourly forecasts are tested against irradiance data from each station of the SURFRAD network (SURFRAD, 2010) including Desert Rock, Nevada; Fort peck, Montana; Boulder, Colorado; Sioux Falls, South Dakota; Bondville, Illinois; Goodwin Creek, Mississippi; and Penn State, Pennsylvania.

These stations cover several distinct climatic environments ranging from arid (Desert Rock) to humid continental locations (Penn State) and from locations with some subtropical influence (Goodwin Creek) to the northern Great Plains (Fort Peck). Boulder is a challenging site for all types of solar radiation models, because of its high elevation (~2000 m) and of its position at the Rocky Mountains' eastern edge, at the junction between two weather regimes.

The present validation period spans a little over one year from August 23, 2008 to August 31, 2009.

3. 1.1. Validation metrics

In addition to the standard Mean Bias and Root Mean Square errors (respectively RMSE and MBE) resulting from the direct comparison between hourly forecasts and hourly measurements, we also consider two metrics that quantify the ability of a model to reproduce observed frequency distributions. The first of these is the Kolmogorov-Smirnoff test Integral (KSI) goodness of fit test (Espinar et al., 2009) recommended by the International Energy Agency Solar Heating & Cooling Programme Task 36 for data benchmarking (Task 36, report, 2010). The KSI metric is obtained by integrating the absolute difference between the measured and modeled cumulative frequency distributions of the considered variable as illustrated in Fig. 1. The second, termed OVER , is calculated by integrating the absolute difference between the measured distribution and the measured distribution plus or minus a buffer determined by the Kolmogorov-Smirnov critical V_c approximated here by (NIST, 2010):

$$V_c = 1.63 / \sqrt{n}$$

where n is the number of consider data points.

Both the KSI and OVER metrics are quantified here as fractions of the critical value.

3. 1.2 Persistence Benchmarking

The single site performance of the forecast models is evaluated by comparing it to measured persistence; same-day measured persistence is obtained by time extrapolation of measured irradiances using a constant Kt*index. Next-day and multi-day persistences are obtained by extrapolating the previous day's mean daily measured Kt*.

3. 1.3 Results

Tables 1 and 2 report respectively the MBEs and RMSEs observed at all sites for all time horizons for the forecast models and persistence benchmarks. Results are reported yearly as well as seasonally. Forecasts include 1 to 6 hours cloud motion forecasts and same-day to 6-day-ahead NDFD forecasts. The satellite model's MBEs and RMSEs are also included in Table 1 and 2 as an additional performance reference.

All forecasts are validated against the same set of experimental values. Hence, because six-hour cloud motion forecasts cannot be generated until the sun is up, the experimental "common validation denominator pool" is limited to points six hours after sunrise.

Figure 2 summarizes the results of Table 2, plotting the yearly RMSE trend for all sites and all models as a function of the forecast time horizon. The satellite model's RMSE is included as a reference and appears as a horizontal line across all forecasts horizons.

Figure 3 provides an illustrative sample of measured vs. model scatter plots at four of the seven sites, including Bondville, Boulder, Desert Rock and Goodwin Creek. This sample includes the reference

satellite model, the one and three-hour cloud-motion forecasts, the next day and three-days-ahead NDFD forecasts, as well as the same time horizons for the measured persistence benchmarks.

Table 3 and Table 4 report the annual KSI and OVER Statistics for all sites, forecast time horizons, satellite reference, and persistence benchmarks.

3.1.4 Discussion

The NDFD-NWP forecasts analyzed here lead to results which are largely consistent with initial evaluations (Perez et al., 2007, Remund et al., 2008). This is an important result, because these initial evaluations only covered a limited period spanning summer months only.

When considering the RMSE metric, it is remarkable to observe that the performance of the one and two-hour cloud motion forecasts is comparable to that of the satellite model from which they are extracted. The one-hour forecasts actually have a lower RMSE than the satellite model at all sites but Boulder: despite the loss of deterministic information due to cloud motion, the image smoothing inherent to the forecasts -- via convergence and divergence of motion vectors, and additional post-processing pixel averaging -- results in lowering the RMSE that quantify short term accuracy. Hence, in effect, lowering the resolution of the satellite model increases its short term accuracy. A corollary of this is that attempting to achieve better short-term accuracy for satellite models by increasing spatial resolution might be illusory given the satellite navigation errors and parallax uncertainties (cloud shadowing, sun/satellite angles) if these uncertainties are not specifically addressed via more complex models. Note that this pixel-averaging performance improvement technique is known and has been previously discussed, e.g., by Stuhlmann et al. (1990) when developing his physical satellite-to-irradiance model.

Cloud motion forecasts are always better than persistence forecasts derived from actual measurements, even after a little as one hour.

The break-even point between cloud motion and NDFD forecasts is between 5 and 6 hours ahead. We note, however, that satellite-aided multiple output statistics (MOS) real-time feedback (e.g., see Dennstaedt, 2006), whereby in the present case the numerical weather forecasts would be corrected from the most recent satellite-derived irradiance history, could improve the NDFD forecasts. Such a feed-back process has not been implemented here.

The cloud motion forecasts' MBE is consistently small, to the exception of sites experiencing important winter snow cover where the accuracy of the current satellite model, relying solely on the visible channel, is limited – a new model proposed by the authors and utilizing the infrared as well as the visible channels of eliminates such bias (Perez et al., 2010); however the model is not yet operational as of this writing.

The NDFD bias exhibits a seasonal pattern as well as site dependence: the bias is smallest for the sites that experience either little cloud cover or fast passing frontal type cloud cover (Western US and Great Plains). The easternmost sites, Penn State and Goodwin Creek, where localized cloud formation is more frequent, exhibit a tendency to negative bias. The seasonal pattern shows a tendency of NDFD forecasts towards positive irradiance bias in the fall (cloudiness underprediction) and negative bias in the other seasons, particularly in the spring (cloudiness overprediction). Despite these shortcomings, the NDFD forecast perform considerably better than persistence up to seven days ahead.

When considering KSI and OVER statistics it is not surprising to observe that the persistence-based forecasts tend to score better than the forecast models. For the short term, same-day forecasts, the statistical distribution of persistence forecasts should be almost identical to measurements' (since they are measurements themselves, albeit time-extrapolated) hence exceed the performance of the satellite

model and of its derived forecasts. One exception is Boulder, CO, where the very marked diurnal patterns at that site produce different statistical distributions for different times of day and where the cloud motion provides better results. The 1-6 days ahead persistence forecast also exhibit a better performance than the NDFD when assessed via the KSI and OVER metrics. As for cloud motion, the NDFD performance statistics deteriorate sensibly with the time horizon, reflecting a loss of dynamic range for both. This is due to pixel convergence/averaging in the case of cloud motion, and likely due to the tendency avoid extreme forecasts (clear or cloudy) as the time horizon increases for the NDFD models.

Fortunately, the KSI and OVER metrics are largely relevant to microclimatological site-characterization and are not critical for forecast operations where the short term accuracy (RMSE) is the key performance factor.

3.2 Extended-area validations

This validation is largely qualitative and focuses on the ability of the forecast models to account for the solar resource's microclimatic features over a given period. The validation criterion is a visual evaluation of mapped solar resource computed from ongoing forecast data. Because we do not dispose of gridded instrumentation spanning the considered areas, we rely on satellite-derived irradiances data as a performance benchmark.

We considered 2^{o} x 2^{o}degree regions (~ 15,000 sq. km) surrounding each ground-truth station. The results are illustrated by presenting the case of Boulder and Desert Rock, which have the strongest (orography-driven) microclimatic features. Figure 4 compares the mapped irradiances for Desert Rock in summer and for Boulder in the fall, spring and year-around. The maps consist of the satellite model, the one and three-hours cloud motion forecasts and the next day, three days, and six days-ahead forecasts. The orographic features that influence solar resource microclimates may be seen in Figure 5.

The NDFD model does account for orography-driven microclimates, but, apparently, only when cloudiness increases with elevation. This underlying assumption holds in Desert Rock in summer and in the spring time in Boulder. However in the fall of 2008 clouds preferentially formed immediately east of the Rocky Mountains likely linked to the presence of easterly winds “upslope” cloud formation. This preferential cloud formation trend was not taken in account by the NDFD models.

The smoothing effect of the cloud motion tends to erase some of the terrain features (pixel convergence and averaging).

Finally, Figure 4 also shows the discontinuities inherent to the NDFD process, whereby global forecasts are modified independently by regional offices before being reassembled on the NDFD grid. The discontinuity at the top of the Boulder maps (appearing as a horizontal discontinuity) marks the boundary between two US National Weather Service offices which produce a different assessment of local cloudiness that becomes apparent over integrated time scales.

4. CONCLUSIONS

The numerical weather prediction-based irradiance forecast analyzed here lead to results which are consistent with our previous limited evaluations. The present validations include a more diverse set of climatic environments and include winter months when models performance tends to be poorer then in summer.

All the considered short-term and long-term forecasts perform significantly better than persistence from actual high accuracy measurements. Satellite-derived cloud motion-based forecasting leads to a significant improvement over NDFD forecasts up to five hours ahead. One-hour forecasts are on par or slightly better than the satellite model from which they are derived; the probable reason is that the

cloud motion methodology results in a smoothing of the predicted images which tends to mitigate satellite's navigation and parallax uncertainties. A corollary of this maybe that the short-term accuracy of satellite models may not be improved significantly by increased image resolution – of course this comment applies only to short-term data and does not pertain to long-term means and the delineation of solar microclimates, where high resolution would be beneficial.

GLOSSARY

ECMWF: European Center for Medium-Range Weather Forecasts

GFS: NOAA'S Global Forecasting System

GHI: Global Horizontal Irradiance

GHI_{clear}: Clear Sky Global Horizontal Irradiance

KSI: Kolmogorov-Smirnov test Integral

Kt*: GHI Index equal to GHI/GHI_{clear}

MBE: mean Bias Error

MOS: Model Output Statistics

NDFD: National Digital Forecast Data Base

NOAA: National Oceanic and Atmospheric Administration

NWP: Numerical Weather Prediction

OVER: That part of the KSI which integrates above (over) the critical value V_c

RMSE: Root Mean Square Error

V_c : Kolmogorov-Smirnov critical value

WRF: Weather Research Forecasting model

ACKNOWLEDGEMENT

The forecast modeling capability was developed as part of the construction of SolarAnywhere® under funding from Clean Power Research. The present validation analysis performed under funding from NREL (contract AEK98833801)

Note from the author: The first author of this paper and his team at the University at Albany receives funding from Clean Power Research to develop and produce the Solar Anywhere solar resource satellite and forecast data evaluated in this paper.

7. REFERENCE

1. SolarAnywhere(2010): Clean Power Research, www.solaranywhere.com
2. NDFD, the National Forecast Database, (2010): National Weather Service, NOAA, Washington, DC. http://www.weather.gov/ndfd/
3. The GFS Model, (2003): Environmental Modeling Center, NOAA, Washington, DC. http://www.emc.ncep.noaa.gov/gmb/moorthi/gam.html
4. ECMWF (2010): European Centre for Medium-Range Weather Forecasts. http://www.ecmwf.int/
5. WRF (2010): Weather research and forecasting (WRF) model. http://www.wrf-model.org
6. Slater D. W., C. N. Long and T. P. Tooman, (2001): Total Sky Imager/Whole Sky Imager Cloud Fraction Comparison. Eleventh ARM Science Team Meeting Proceedings, Atlanta, Georgia, March 19-23, 2001
7. Perez R., P. Ineichen, K. Moore, M. Kmiecik, C. Chain, R. George and F. Vignola, (2002): A New Operational Satellite-to-Irradiance Model. Solar Energy 73, 5, pp. 307-317
8. Perez R., P. Ineichen, M. Kmiecik, K. Moore, R. George and D. Renne, (2004): Producing satellite-derived irradiances in complex arid terrain. Solar Energy 77, 4, 363-370

9. Lorenz, E., D. Heinemann, H. Wickramarathne, H.G. Beyer and S. Bofinger, (2007): Forecast of Ensemble Power production by Grid-connected PV Systems, Proc. 20th European PV Conference, Milano, Italy

10. Xu, K. M., and D. A. Randall, (1996): A semiempirical cloudiness parameterization for use in climate models. J. Atmos. Sci., 53, 3084-3102.

11. Perez, R., K. Moore, S. Wilcox, D. Renné, and A. Zelenka, (2007): Forecasting Solar Radiation – Preliminary Evaluation of an Approach Based upon the national Forecast Data Base. Solar Energy 81, 6, pp. 809-812

12. The SURFRAD Network (2010): Monitoring Surface Radiation in the Continental United States. National Weather Service, NOAA, Washington, DC.

13. Espinar, B., L. Ramírez, A. Drews, H.G. Beyer, L.F. , Zarzalejo, J. Polo, L. Martín, (2008): Analysis of different error parameters applied to solar radiation data from satellite and German radiometric stations, Solar Energy, Volume 83, Issue 1, January 2009

14. IEA-SHCP task 36, (2010): Final Report, Subtask A - Standard Qualification for Solar Resource Products

15. NIST, National Institute of Standards and Technology, (2010): Engineering and Statistics Handbook. www.itl.nist.gov

16. Remund J., R. Perez and E. Lorenz, (2008): Comparison of Solar Radiation Forecasts for the USA. Proc. of 23rd European PV Conference, Valencia, Spain.

17. Stuhlmann, R., Rieland, M. and Raschke, E., (1990): An improvement of the IGMK model to derive total and diffuse solar radiation at the surface from satellite data. J. appl. Meteorol. 29, pp. 586–603

18. Dennstaedt, S., (2006): Model Output Statistics Provide Essential Data for Small Airports, The Front, 6, 2, pp. 1-4.

19. Perez R., S. Kivalov, A. Zelenka, J. Schlemmer and K Hemker Jr., (2010): Improving the Performance of Satellite-to-Irradiance Models Using the Satellite's Infrared Sensors. Proc. of American Solar Energy Society's Annual Conference, Phoenix, AZ.

List of Figures:

List of Tables:

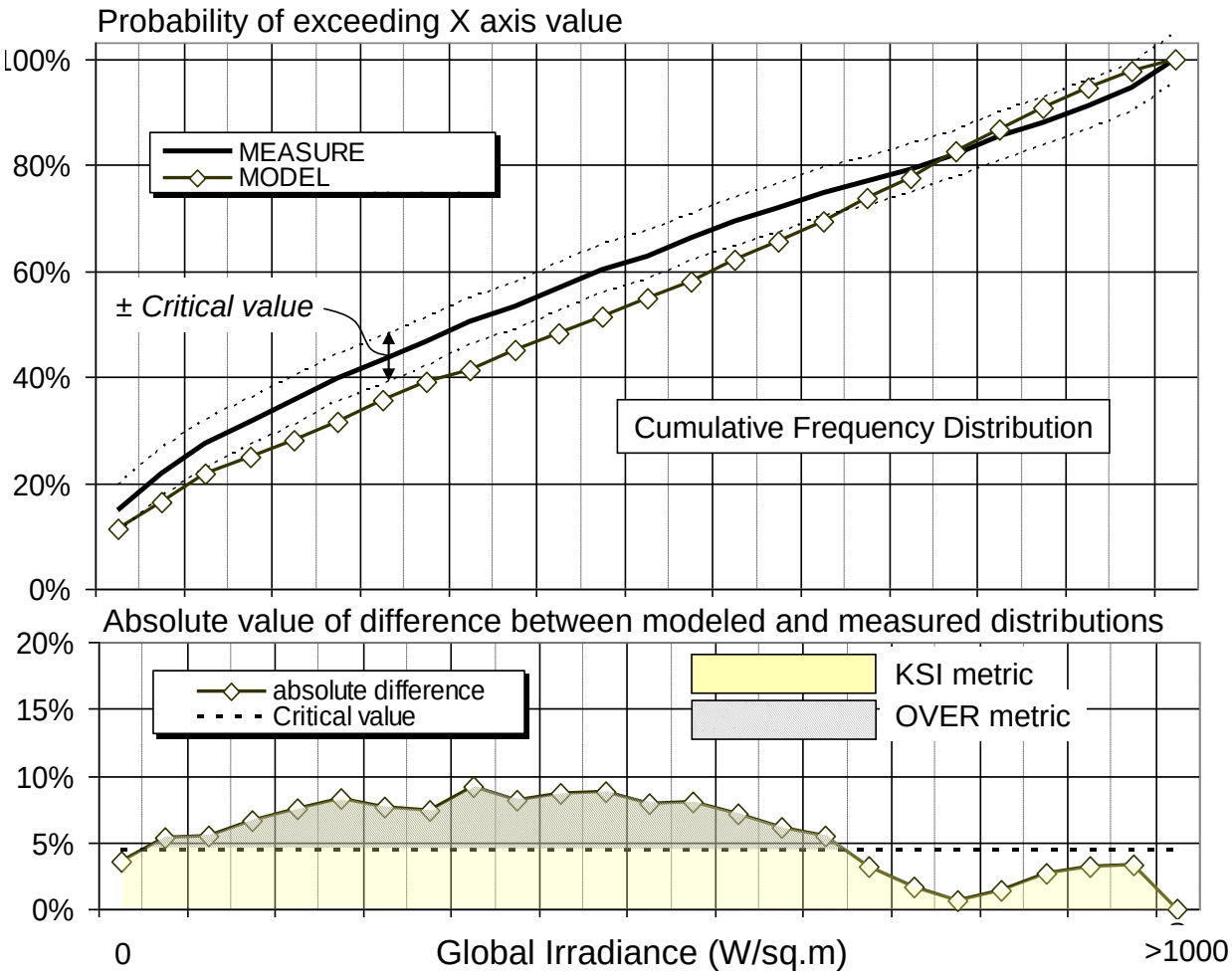

Figure 1: Illustration of KSI and OVER validation metrics. The top graph shows the modeled and measured cumulative probability distributions and the critical value envelope around the latter. The bottom graph plots the absolute difference between the two distributions from which the metrics are obtained by integration (lightly shaded area for the KSI metric and striped area for the OVER metric)

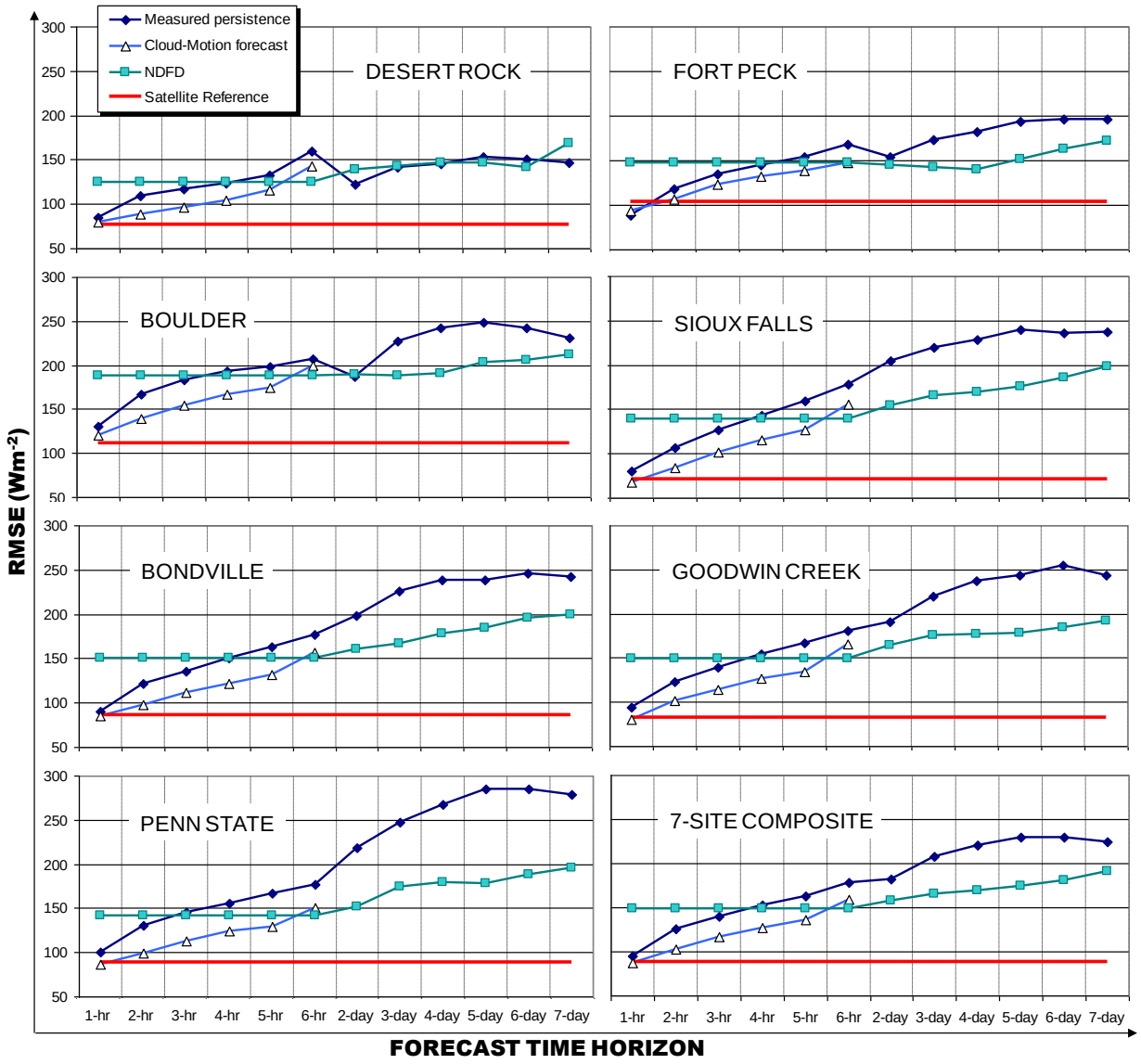

Figure 2: Annual RMSEs as a function of forecast time horizon

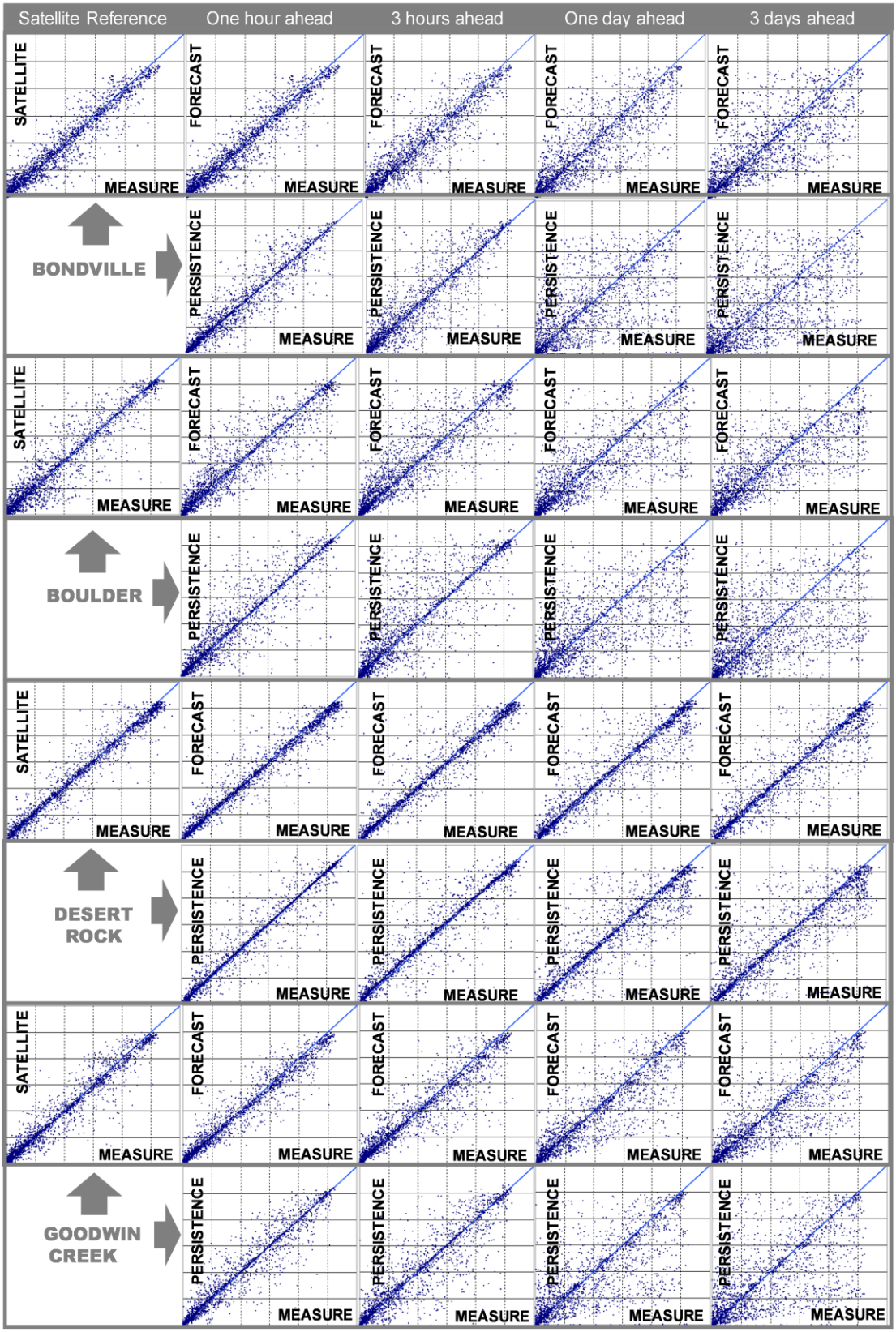

Figure 3: Hourly forecasts and persistence vs. measured GHI for 1, 3 hours and 1, 3-days ahead

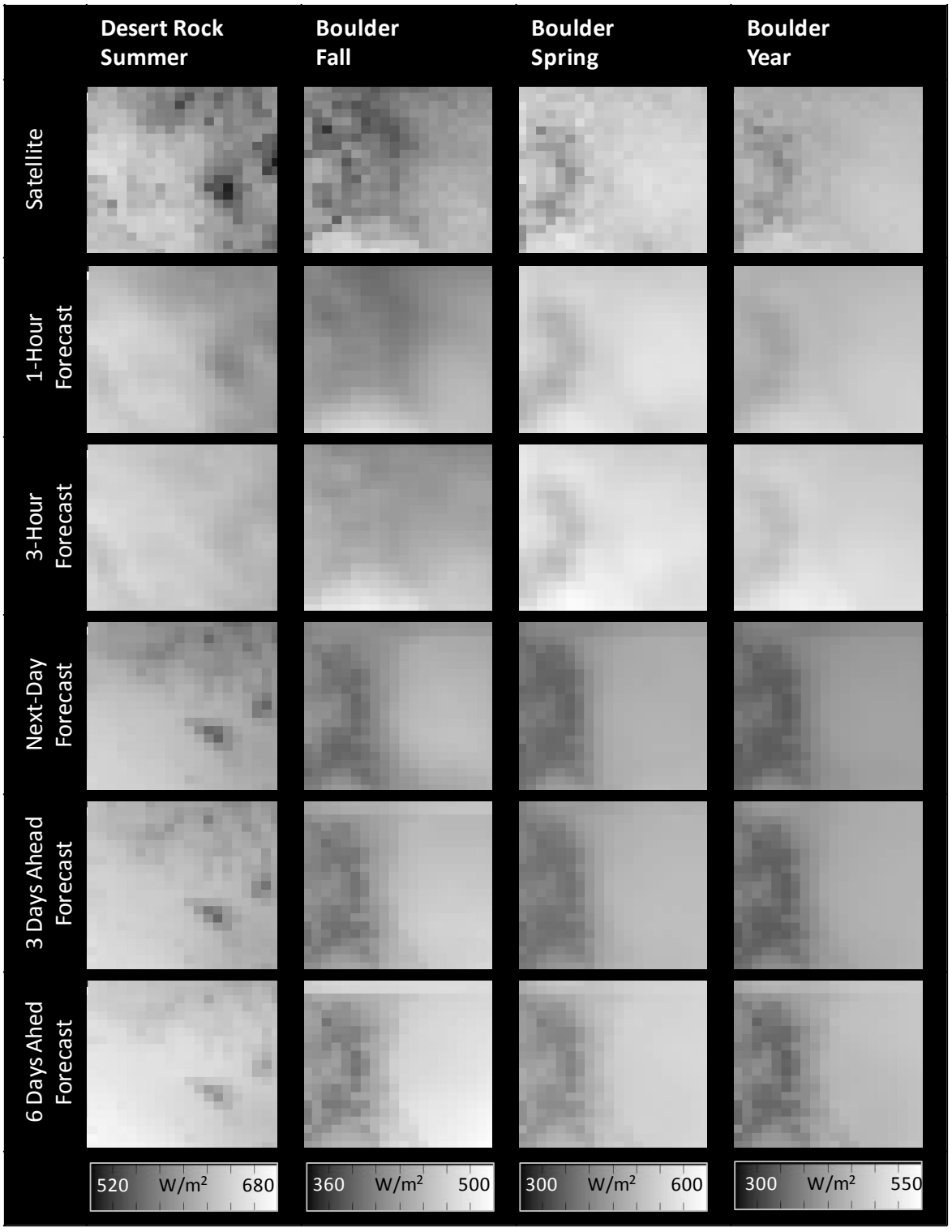

Figure 4: long term average GHI from in a 2o x 2o region surrounding the sites of Boulder and Desert Rock, for the satellite model, cloud motion forecasts (1 &3 hours ahead) and NDFD forecasts (1, 3 and 6 days ahead)

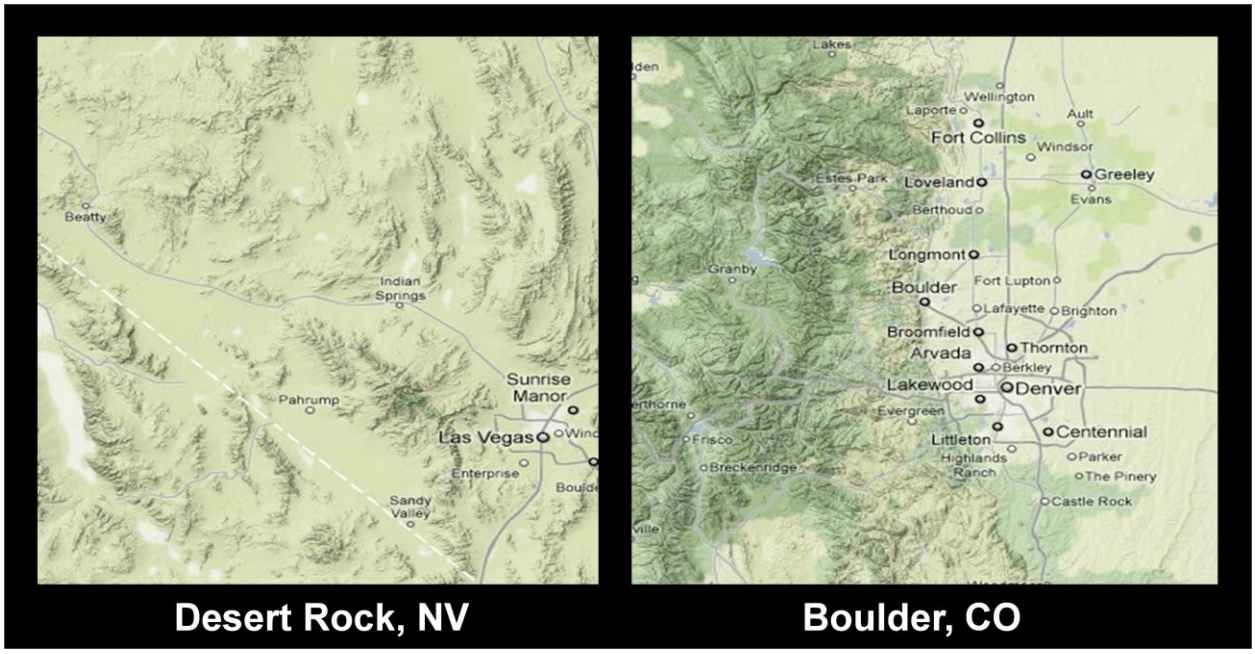

Figure 5: Illustration of the orographic features in the regions analyzed in Fig. 4

TABLE 1: Yearly and seasonal MBE Metric Summary

	MBE	Desert Rock		Fort Peck		Boulder		Sioux Falls		Bondville		Gdwn Creek		Penn State	
ALL YEAR	Mean Obeserved GHI	498		357		369		364		349		397		323	
	Clearness index*	90%		75%		71%		76%		69%		76%		66%	
	Satellite Model error	1		-4		7		14		-3		-1		4	
	Forecast/ persistence	**Fcst**	**Prst**	**Fcst**	**Prst**	**Fcst**	**Prst**	**Fcst**	**Prst**	**Fcst**	**Prst**	**Fcst**	**Prst**	**Fcst**	**Prst**
	1-hour ahead	1	11	-3	8	13	20	15	7	-2	6	-5	6	-4	5
	2-hours ahead	2	18	0	12	26	36	13	11	-3	11	-8	7	-7	6
	3-hours ahead	5	20	-3	13	33	47	9	10	-3	15	-13	4	-7	5
	4-hours ahead	5	16	-5	10	36	50	3	4	-2	17	-20	-3	-4	-3
	5-hours ahead	1	3	-7	2	38	44	0	-7	-3	12	-19	-14	-2	-16
	6-hours ahead	-13	-23	-6	-13	38	28	-7	-19	0	3	-28	-31	-2	-32
	1-Day (Same day)	-5		13		-22		-12		-14		-33		-28	
	2-Day (Next Day)	-10	0	12	-2	-25	1	-17	-2	-19	-3	-35	-3	-30	-1
	3-Day	-16	0	14	-2	-23	0	-18	-3	-15	-1	-46	-4	-40	-2
	4-Day	-12	-1	17	-2	-14	2	-14	-2	-14	-1	-48	-4	-35	-2
	5-Day	-7	-1	22	-3	-7	0	-8	-1	-13	-1	-51	-4	-36	-3
	6-Day	1	-1	24	-4	-6	-2	-13	-2	-14	-1	-48	-4	-40	-3
	7-Day	-30	-2	11	-4	-11	-2	-17	-2	-17	2	-43	-5	-48	-4
WINTER	Mean Obeserved GHI	236		159		215		160		137		189		140	
	Clearness index*	82%		51%		78%		77%		73%		72%		73%	
	Satellite Model error	12		-49		18		23		32		17		47	
	1-hour ahead	11	14	-63	10	14	11	9	8	17	5	7	10	27	6
	2-hours ahead	10	23	-66	15	7	20	0	14	9	9	6	11	16	10
	3-hours ahead	11	28	-70	17	-1	24	-9	17	0	11	3	5	12	13
	4-hours ahead	13	26	-72	13	-7	23	-15	15	2	13	2	0	12	12
	5-hours ahead	12	17	-69	5	-11	12	-17	8	4	11	3	-7	21	5
	6-hours ahead	7	0	-60	-5	-23	-2	-25	-1	25	2	11	-25	18	-9
	1-Day (Same day)	-13		-47		-37		-39		-15		-9		-44	
	2-Day (Next Day)	-15	6	-34	3	-31	5	-41	5	-21	3	-13	6	-37	3
	3-Day	-20	5	-26	1	-38	8	-33	8	-7	11	-23	7	-33	6
	4-Day	-28	3	-22	3	-34	8	-24	12	-7	11	-26	5	-27	9
	5-Day	-30	2	-19	4	-34	10	-8	11	6	14	-25	10	-30	6
	6-Day	-30	1	-22	7	-36	8	-1	9	9	6	-16	11	-30	3
	7-Day	-31	2	-24	9	-40	6	0	8	17	8	-14	15	-37	3
SPRING	Mean Obeserved GHI	548		377		416		391		373		416		361	
	Clearness index*	90%		72%		68%		73%		65%		72%		64%	
	Satellite Model error	7		-3		-1		11		-2		1		3	
	1-hour ahead	5	14	2	13	12	21	18	7	8	7	-4	4	0	8
	2-hours ahead	7	22	7	21	20	35	18	11	5	12	-13	4	1	9
	3-hours ahead	12	26	4	24	20	42	15	11	9	16	-24	-6	1	5
	4-hours ahead	11	25	0	23	18	41	6	6	6	15	-37	-19	1	-7
	5-hours ahead	5	13	-6	17	17	31	3	-5	5	9	-37	-34	1	-25
	6-hours ahead	-6	-11	4	4	4	8	2	-16	16	-2	-37	-51	7	-46
	1-Day (Same day)	-6		10		-35		-18		-17		-63		-20	
	2-Day (Next Day)	-15	1	0	-2	-40	5	-26	-3	-23	-12	-46	-5	-35	-4
	3-Day	-28	4	-2	-4	-46	5	-38	-8	-23	-10	-50	-10	-42	-6
	4-Day	-21	8	1	-5	-33	6	-35	-8	-28	-10	-68	-13	-44	-3
	5-Day	-18	9	3	-7	-13	5	-30	-7	-25	-3	-56	-14	-42	0
	6-Day	-9	10	9	-8	-12	10	-35	-6	-34	2	-51	-12	-47	6
	7-Day	-41	8	4	-9	-20	12	-29	-1	-49	8	-57	-8	-62	12
SUMMER	Mean Obeserved GHI	617		454		432		451		443		510		403	
	Clearness index*	90%		80%		70%		79%		70%		81%		66%	
	Satellite Model error	-7		-3		4		12		-19		-8		-15	
	1-hour ahead	-6	9	2	3	11	21	13	7	-19	5	-8	3	-20	3
	2-hours ahead	-3	15	7	4	34	40	12	7	-15	11	-9	4	-23	4
	3-hours ahead	-1	13	4	4	55	58	9	3	-14	16	-12	4	-21	3
	4-hours ahead	-2	5	4	-2	67	66	6	-5	-10	19	-18	1	-13	-6
	5-hours ahead	-9	-13	3	-12	76	64	3	-19	-13	14	-19	-10	-12	-20
	6-hours ahead	-28	-49	-2	-28	68	52	-8	-30	-16	6	-41	-24	-10	-30
	1-Day (Same day)	-15		18		-42		-13		-24		-21		-45	
	2-Day (Next Day)	-22	0	23	-4	-53	2	-15	-1	-27	-4	-36	-8	-40	0
	3-Day	-24	0	29	-7	-41	4	-7	-2	-23	-5	-60	-10	-68	-1
	4-Day	-19	0	31	-7	-31	9	-3	1	-21	-5	-51	-14	-52	0
	5-Day	-8	0	39	-8	-30	8	0	3	-28	-4	-68	-14	-55	2
	6-Day	7	0	38	-9	-35	3	-23	4	-29	0	-72	-12	-63	4
	7-Day	-46	1	10	-6	-40	2	-49	5	-35	5	-60	-12	-61	2
FALL	Mean Obeserved GHI	406		246		291		250		265		327		253	
	Clearness index*	90%		76%		72%		72%		70%		76%		69%	
	Satellite Model error	0		24		15		18		6		1		11	
	1-hour ahead	2	11	17	10	20	20	17	9	3	8	-7	11	1	4
	2-hours ahead	2	16	14	13	29	34	16	15	4	15	-9	13	-3	6
	3-hours ahead	3	19	10	13	32	41	11	19	6	22	-14	14	-5	5
	4-hours ahead	5	19	6	7	30	42	7	17	8	26	-15	10	-2	1
	5-hours ahead	4	7	2	-1	26	37	4	10	9	21	-13	-2	-1	-12
	6-hours ahead	-14	-16	-7	-18	8	22	-7	-7	0	13	-24	-19	-7	-30
	1-Day (Same day)	20		33		41		13		10		-17		6	
	2-Day (Next Day)	21	0	30	-6	37	3	6	2	10	-3	-18	-6	7	3
	3-Day	18	1	26	-7	38	4	2	2	14	-6	-21	-10	6	6
	4-Day	22	1	31	-5	46	6	0	6	21	-5	-22	-13	13	9
	5-Day	24	2	31	-5	51	9	15	9	27	-5	-26	-14	12	9
	6-Day	21	4	35	-1	63	10	30	10	33	-3	-25	-13	17	12
	7-Day	11	5	36	-3	59	5	62	13	45	0	-23	-13	3	15

** GHI/GHIclear*

TABLE 2: Yearly and seasonal RMSE Metric Summary

	RMSE	Desert Rock		Fort Peck		Boulder		Sioux Falls		Bondville		Gdwn Creek		Penn State	
ALL YEAR	Mean Obeserved GHI	498		357		369		364		349		397		323	
	Clearness index*	90%		75%		71%		76%		69%		76%		66%	
	Satellite Model error	77		103		112		72		87		83		89	
	Forecast/ persistence	**Fcst**	**Prst**	**Fcst**	**Prst**	**Fcst**	**Prst**	**Fcst**	**Prst**	**Fcst**	**Prst**	**Fcst**	**Prst**	**Fcst**	**Prst**
	1-hour ahead	80	85	94	88	120	130	68	80	85	91	80	93	86	100
	2-hours ahead	88	109	106	118	139	167	84	106	98	122	101	123	99	131
	3-hours ahead	96	118	123	135	154	183	102	127	112	135	114	139	113	145
	4-hours ahead	104	123	132	145	166	193	115	142	122	150	127	154	124	155
	5-hours ahead	116	133	138	154	175	199	126	159	132	164	134	166	129	166
	6-hours ahead	142	160	147	168	200	207	155	178	156	177	166	181	150	176
	1-Day (Same day)	125		148		188		140		151		149		141	
	2-Day (Next Day)	139	122	145	154	189	187	155	205	161	199	164	191	152	218
	3-Day	142	141	142	174	188	227	165	220	167	226	176	219	174	247
	4-Day	147	145	140	181	191	242	170	229	178	238	177	237	179	267
	5-Day	147	152	151	194	203	249	176	240	184	239	178	243	179	285
	6-Day	141	150	162	196	206	242	186	235	196	246	185	254	188	284
	7-Day	169	147	172	196	212	231	198	238	200	243	193	243	196	278
WINTER	Mean Obeserved GHI	236		159		215		160		137		189		140	
	Clearness index*	82%		51%		78%		77%		73%		72%		73%	
	Satellite Model error	53		126		74		52		76		53		76	
	1-hour ahead	46	53	107	26	64	53	48	36	60	52	48	53	57	42
	2-hours ahead	48	65	105	37	71	71	58	54	66	61	59	67	57	59
	3-hours ahead	59	78	109	44	81	82	69	68	74	73	66	80	59	64
	4-hours ahead	70	84	112	50	85	87	78	80	81	81	70	87	65	67
	5-hours ahead	74	88	115	58	89	93	76	83	79	82	80	92	71	66
	6-hours ahead	85	94	117	67	108	98	96	83	102	83	110	101	90	68
	1-Day (Same day)	102		122		130		112		91		84		94	
	2-Day (Next Day)	114	137	98	117	117	144	100	133	105	132	99	133	94	109
	3-Day	107	153	93	99	125	141	111	125	88	136	121	147	111	143
	4-Day	125	163	81	108	127	149	105	148	121	164	121	162	103	148
	5-Day	126	170	85	105	137	170	102	138	84	150	128	157	112	145
	6-Day	128	167	94	117	136	154	101	135	97	149	119	163	101	141
	7-Day	133	151	100	99	143	151	108	130	106	127	126	175	112	130
SPRING	Mean Obeserved GHI	548		377		416		391		373		416		361	
	Clearness index*	90%		72%		68%		73%		65%		72%		64%	
	Satellite Model error	68		117		129		74		93		86		85	
	1-hour ahead	86	97	110	88	125	126	69	84	93	101	92	115	83	99
	2-hours ahead	95	139	124	119	141	165	90	112	109	136	122	152	99	136
	3-hours ahead	111	143	141	135	157	175	107	135	123	145	144	178	118	154
	4-hours ahead	115	142	148	146	170	186	126	150	137	159	164	199	137	168
	5-hours ahead	127	147	155	157	180	199	133	166	151	175	174	209	143	182
	6-hours ahead	152	166	160	172	219	217	171	180	181	188	198	226	162	194
	1-Day (Same day)	139		154		195		136		164		186		143	
	2-Day (Next Day)	154	134	161	159	199	222	153	236	168	239	203	231	156	263
	3-Day	159	154	150	190	196	275	184	253	176	276	203	269	173	292
	4-Day	163	154	147	199	209	277	189	262	172	298	207	274	184	308
	5-Day	166	165	153	206	231	284	194	281	193	288	203	284	182	328
	6-Day	160	171	170	223	245	273	207	277	219	293	217	301	191	322
	7-Day	180	177	177	225	251	259	214	294	228	306	228	276	205	326
SUMMER	Mean Obeserved GHI	617		454		432		451		443		510		403	
	Clearness index*	90%		80%		70%		79%		70%		81%		66%	
	Satellite Model error	99		99		124		80		100		97		113	
	1-hour ahead	99	100	91	111	143	170	80	97	100	108	92	103	112	131
	2-hours ahead	110	119	109	149	175	214	98	127	115	145	113	135	127	164
	3-hours ahead	111	132	129	169	189	233	120	150	129	160	120	145	142	181
	4-hours ahead	124	144	142	180	204	245	129	167	138	178	129	157	152	191
	5-hours ahead	138	157	150	188	212	246	148	190	150	197	131	175	155	204
	6-hours ahead	169	199	160	204	224	252	176	217	167	217	170	190	183	213
	1-Day (Same day)	146		167		221		171		178		146		176	
	2-Day (Next Day)	165	133	159	173	228	197	192	229	193	216	171	204	186	234
	3-Day	170	154	165	196	225	241	184	243	204	227	194	225	222	268
	4-Day	172	155	164	207	217	277	194	249	222	221	193	259	225	299
	5-Day	170	169	181	220	221	290	201	264	226	227	196	241	223	319
	6-Day	154	164	189	213	221	284	212	258	231	264	198	247	237	325
	7-Day	204	174	202	212	229	280	233	254	228	254	207	240	237	322
FALL	Mean Obeserved GHI	406		246		291		250		265		327		253	
	Clearness index*	90%		76%		72%		72%		70%		76%		69%	
	Satellite Model error	62		70		80		63		59		65		60	
	1-hour ahead	55	56	59	62	85	84	49	52	58	63	55	58	60	70
	2-hours ahead	62	67	67	76	97	112	54	69	68	89	66	81	71	92
	3-hours ahead	69	74	83	93	110	131	64	86	84	107	81	93	76	96
	4-hours ahead	72	78	88	103	120	142	80	100	89	116	94	109	83	109
	5-hours ahead	83	91	92	115	129	148	90	114	97	115	102	119	91	118
	6-hours ahead	113	111	114	130	159	150	110	134	128	116	144	132	102	132
	1-Day (Same day)	81		100		141		86		96		116		99	
	2-Day (Next Day)	77	69	102	127	135	146	91	133	108	158	106	144	109	178
	3-Day	83	84	95	142	136	181	121	160	112	209	117	179	119	182
	4-Day	88	87	93	152	149	179	115	171	124	209	121	195	125	174
	5-Day	85	87	102	151	158	183	126	175	133	194	126	195	125	194
	6-Day	92	82	111	147	155	195	129	151	143	197	147	202	123	205
	7-Day	103	79	116	156	156	164	134	159	141	203	152	205	138	196

TABLE 3: Annual KSI Metric Summary

KSI	Desert Rock		Fort Peck		Boulder		Sioux Falls		Bondville		Gdwn Creek		Penn State		All Sites	
Satellite Model error	23%		19%		21%		30%		55%		43%		40%		33%	
Forecast/ persistence	**Fcst**	**Prst**	**Fcst**	**Prst**	**Fcst**	**Prst**	**Fcst**	**Prst**	**Fcst**	**Prst**	**Fcst**	**Prst**	**Fcst**	**Prst**	**Fcst**	**Prst**
1-hour ahead	39%	19%	13%	18%	62%	45%	32%	15%	56%	13%	56%	16%	56%	10%	45%	20%
2-hours ahead	37%	33%	20%	26%	84%	86%	32%	23%	58%	16%	66%	21%	60%	11%	51%	31%
3-hours ahead	39%	43%	15%	29%	102%	112%	45%	23%	58%	30%	82%	28%	62%	13%	58%	40%
4-hours ahead	47%	51%	18%	20%	109%	125%	63%	32%	57%	36%	97%	33%	66%	29%	65%	47%
5-hours ahead	55%	60%	22%	22%	121%	118%	81%	48%	71%	24%	103%	58%	77%	55%	76%	55%
6-hours ahead	71%	94%	28%	47%	117%	102%	90%	65%	81%	22%	138%	97%	83%	89%	87%	74%
	64%		61%		89%		43%		59%		108%		70%			
2-Day (Next Day)	65%	64%	63%	55%	117%	104%	66%	49%	74%	67%	113%	117%	75%	72%	82%	76%
3-Day	69%	66%	65%	55%	123%	105%	70%	52%	75%	65%	139%	121%	99%	77%	92%	77%
4-Day	62%	65%	76%	58%	140%	106%	70%	51%	82%	64%	144%	122%	89%	82%	95%	78%
5-Day	61%	63%	87%	55%	145%	106%	86%	49%	93%	64%	156%	122%	97%	83%	104%	77%
6-Day	63%	63%	99%	54%	159%	107%	121%	53%	106%	58%	151%	121%	115%	82%	116%	77%
7-Day	67%	62%	104%	53%	161%	108%	137%	51%	121%	56%	146%	122%	134%	82%	124%	76%

TABLE 4: Annual OVER Metric Summary

OVER	Desert Rock		Fort Peck		Boulder		Sioux Falls		Bondville		Gdwn Creek		Penn State		All Sites	
Satellite Model error	0%		0%		0%		0%		6%		0%		3%		1%	
Forecast/ persistence	**Fcst**	**Prst**	**Fcst**	**Prst**	**Fcst**	**Prst**	**Fcst**	**Prst**	**Fcst**	**Prst**	**Fcst**	**Prst**	**Fcst**	**Prst**	**Fcst**	**Prst**
1-hour ahead	15%	0%	0%	0%	30%	0%	0%	0%	5%	0%	5%	0%	1%	0%	8%	0%
2-hours ahead	10%	0%	0%	0%	60%	58%	10%	0%	10%	0%	10%	0%	0%	0%	14%	8%
3-hours ahead	6%	0%	0%	0%	84%	102%	15%	0%	5%	0%	50%	0%	0%	0%	23%	15%
4-hours ahead	15%	6%	0%	0%	95%	118%	17%	0%	10%	0%	67%	0%	2%	0%	29%	18%
5-hours ahead	19%	26%	0%	0%	102%	107%	58%	0%	36%	0%	84%	21%	8%	0%	44%	22%
6-hours ahead	48%	78%	0%	0%	97%	86%	65%	45%	51%	0%	122%	64%	10%	16%	56%	41%
	19%		25%		67%		0%		0%		81%		8%			
2-Day (Next Day)	25%	25%	40%	22%	103%	88%	34%	10%	31%	15%	85%	95%	3%	5%	46%	37%
3-Day	37%	26%	42%	21%	113%	84%	35%	10%	41%	15%	114%	97%	26%	8%	58%	37%
4-Day	24%	26%	49%	21%	129%	83%	39%	10%	43%	10%	128%	102%	20%	10%	62%	38%
5-Day	18%	26%	59%	21%	135%	83%	64%	5%	67%	10%	139%	102%	25%	10%	72%	37%
6-Day	29%	25%	75%	21%	151%	90%	109%	15%	85%	5%	128%	102%	43%	11%	89%	38%
7-Day	38%	25%	82%	21%	153%	95%	124%	14%	106%	0%	124%	103%	60%	10%	98%	38%